Quantization Noise Cancellation of Fractional-*N* Frequency Synthesizers Using Pre-distortion Technique

Kang-Chun PENG[1], *Yan-Ru LU*[2], *Zhi-Hong HUANG*[3]

[1]Dept. of Computer and Communication Engineering, National Kaohsiung First University of Science and Technology, No. 2 Jhuoyue Rd., Nanzih, Kaohsiung, Taiwan
[2]Chung Shan Institute of Science and Technology, No. 15, Shi Qi Zi, Gaoping village, Taoyuan County, Taiwan, R.O.C.
[3]Syncomm Technology Corp., 6F-15, No. 81, Shui-Li Road, Hsinchu City, Taiwan, R.O.C.

peterpkg@nkfust.edu.tw, angel_nash2000@yahoo.com.tw, ab77889900@msn.com

Abstract. *This work proposes a novel pre-distortion technique for the quantization noise cancellation of fractional-N frequency synthesizers. The proposed technique utilizes the coordinate rotation digital computer (CORDIC) algorithm to pre-distort the baseband signal of a wireless system with the quantization noise. The pre-distorted signal then modulates the noisy output signal of the fractional-N frequency synthesizer. The transmitter (Tx) modulation quality is thereby improved. In the receiver (Rx) mode, the phase noise of the Rx carrier signal can also be improved by modulation with a pre-distorted sinusoidal signal rather than a baseband signal. Experimental results demonstrate that the novel pre-distortion technique effectively improves the modulation quality of a Tx by an error vector magnitude (EVM) of about 10 % under a 13 Mbps QPSK modulation. The carrier in-band and out-band phase noise of the fractional-N frequency synthesizer is improved by approximately 6 dB and 10 dB, respectively.*

Keywords

Fractional-*N* frequency synthesizer, delta-sigma modulation, quantization noise, CORDIC, pre-distortion.

1. Introduction

Wireless communication systems always require high-performance frequency synthesizers to provide stable RF carrier signals for the up-conversion, down-conversion, modulation and demodulation of signals. Since the latest consumer wireless systems, such as smartphones and tablets, apply orthogonal frequency-division multiplexing (OFDM) to provide a high spectral efficiency, the in-band phase noise of the RF carrier signals should be as low as possible [1]. Furthermore, the latest wireless communication systems typically support multiple wireless standards to be flexibly used in various wireless applications. Consequently, the locking time and frequency resolution of frequency synthesizers should be optimized for fast and precise frequency switching, respectively. To achieve these goals, fractional-*N* frequency synthesizers are developed to replace traditional integer-*N* frequency synthesizers [2]-[9].

Most fractional-*N* frequency synthesizers are based on phase-locked loop (PLL) architectures and use a digital delta-sigma modulator (DSM) to quantize the fractional channel selecting information. The quantized results are then used to control the integer multi-modulus divider (MMD). With this architecture, the frequency resolution of the synthesizer increases with the bus width of the DSM. Hence, the division ratio *N* of the synthesizer can be as low as possible to improve both phase noise performance and frequency switching speed [4]-[6]. However, a tradeoff still exists between the phase noise performance and the frequency switching speed. The DSM pushes the quantization noise from the center frequency to a higher offset frequency, and injects this shaped quantization noise into the synthesizer via the MMD. To suppress this quantization noise, the loop bandwidth of the synthesizer must be sufficiently narrow. However, a narrower loop bandwidth results in a longer stable time [6]. To overcome this issue, various quantization noise cancellation techniques have been proposed. In some investigations, the phase-interpolation technique has been used [6], [7]. As the DSM quantizes the fractional information, the digital quantization noise is converted into the analog domain. The analogue quantization noise then phase-interpolates the tuning signal of the voltage-controlled oscillator (VCO) to cancel the quantization noise, which is injected via MMD. Since this architecture requires highly precise digital-to-analog converter (DAC), synchronization mechanism and interpolating circuit for noise cancellation, the circuitry is highly complicated. Accordingly, both the die area and power consumption are increased.

Shekhar used a reference signal with a very high frequency in a fractional-*N* frequency synthesizer [8]. The DSM quantization noise can be pushed to a several hundred MHz offset frequency, which is far away from the loop bandwidth, for noise suppressing. However, the several hundred MHz reference signal should be synthesized by a second PLL and the all-digital DSM also operates at such a high frequency, so the total power consumption is considerable. Wang proposed a pre-distortion technique to eliminate fractional spurs which is caused by the DSM [9]. The technique is based on pre-distorting the DSM inputs by the addition of a series of small sinusoidal signals in anti-phase with the principal fractional spurs. However, this technique eliminates fractional spurs rather than quantization noise. In addition, these fractional spurs should be pre-measured and stored in a read-only-memory (ROM). This means that the architecture requires a high-capacity ROM for storing the pre-distorting information of all channels.

To effectively overcome the tradeoff between the phase noise performance and the frequency switching speed, this work develops a novel pre-distortion technique for quantization noise cancellation. In contrast with the Wang's pre-distortion technique, the proposed pre-distortion technique eliminates the requirement of a high-capacity ROM. The proposed pre-distortion technique is based mainly on the inherent baseband processing and modulation of a wireless system. Hence, the circuitry of the proposed fractional-*N* frequency synthesizer is compact and power-saving. Section 2 presents an overview of the proposed pre-distortion architecture and analyzes the quantization noise cancellation mechanism. Section°3 presents the experimental proof that the proposed technique effectively improves the carrier phase noise and the modulation quality. Finally, conclusions are given in Section 4.

2. Architecture and System Analysis

2.1 Proposed Pre-distortion Architecture

Fig. 1 presents the proposed pre-distortion technique for quantization noise cancellation of fractional-*N* frequency synthesizers. The quantization noise is extracted from the DSM for noise cancellation. In the transmitter (Tx) mode, the baseband signal of a wireless system is pre-distorted by the inverted quantization noise of DSM using a pre-distortion filter. The pre-distorted baseband signal then modulates the noisy RF signal which is produced by the fractional-*N* frequency synthesizer. Since the RF signal has the same quantization noise as the extracted noise, the quantization noise in one signal cancels out that in the other. Therefore, the loop bandwidth of the proposed fractional-*N* frequency synthesizer can be more easily optimized for low phase noise and fast channel-switching than can conventional fractional-*N* frequency synthesizers. The improvement in phase noise consequently improves the Tx modulation quality of the wireless system.

In the receiver (Rx) mode, sinusoidal signals replace the baseband signals for pre-distortion. The pre-distorted sinusoidal signals modulate the RF signal, which is produced by the fractional-*N* frequency synthesizer, to cancel out the quantization noise. Therefore, the modulation yields a low-noise continuous wave (CW) as a perfect carrier signal for use in the Rx of a wireless system.

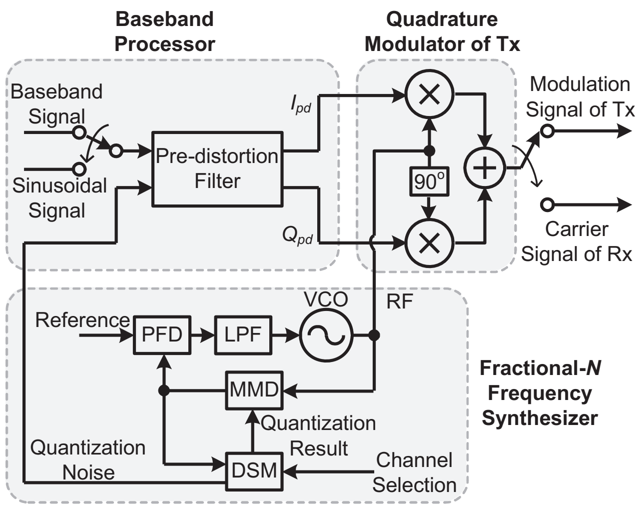

Fig. 1. Proposed pre-distortion technique for quantization noise cancellation of fractional-*N* frequency synthesizers.

2.2 Modified DSM and Extraction of Quantization Noise

To extract quantization noise, a modified second-order DSM is developed. Fig. 2 presents this DSM, where L is the bus width of the accumulator, and $N_1(z)$ and $N_2(z)$ are the overflow of accumulators. The proposed DSM is based on a multi-stage noise-shaping (MASH) architecture. It has one more first-order differentiator than the conventional DSM at the end of the second accumulator to extract the quantization noise.

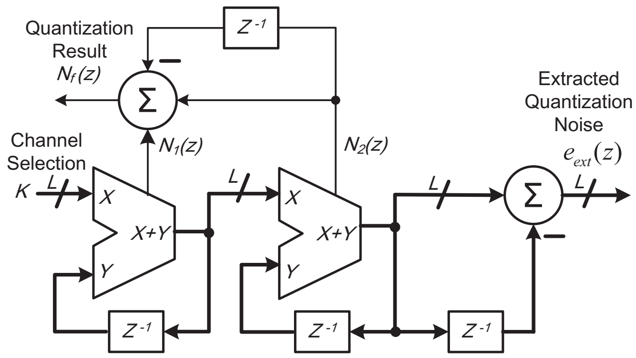

Fig. 2. Modified second-order DSM for extracting quantization noise.

Based on Fig. 2, the quantization result of the proposed DSM is derived as

$$N_f(z) = \frac{K}{2^L} + e_{q2}\left(1 - z^{-1}\right)^2 = \frac{K}{2^L} + e_{DSM}(z) \qquad (1)$$

where $K/2^L$ is the fractional part of the fractional division ratio N; e_{q2} is the original quantization noise, and $(1\text{-}z^{-1})^2$ is the noise shaping factor, which represents a second-order differentiation. The differentiation can push the quantization noise from the center frequency to a high offset frequency. Therefore,

$$e_{DSM}(z) = e_{q2}(1-z^{-1})^2 \tag{2}$$

represents the shaped quantization noise of DSM. Based on Fig. 2, the extracted quantization noise can be derived as

$$e_{ext}(z) = e_{q2}(1-z^{-1}) \tag{3}$$

where the noise shaping order is lower than the one of the shaped quantization noise $e_{DSM}(z)$ by one. The main reason is that the shaped quantization noise $e_{DSM}(z)$ injects into the frequency synthesizer with frequency modulation (FM) [6]. However, the extracted quantization noise $e_{DSM}(z)$ pre-distorts the carrier signal with phase modulation (PM) for noise cancellation. According to the modulation theory, FM can be treated as a combination of first-order integration and PM [10]. This relationship between PM and FM explains why the noise shaping of the extracted quantization noise must be one order lower than that of the shaped quantization noise.

2.3 Noise Cancellation Model and Analysis

Considering the phase noise requirement in both Tx and Rx mode, Fig. 3 presents the phase noise model of the fractional-N frequency synthesizer that is shown in Fig. 1 to analyze the noise cancellation technique. The major noise sources presented in a fractional-N frequency synthesizer mainly include reference crystal, VCO, CP and DSM. Digital circuits such as PFD and divider mainly introduce noises on power and ground, so their contributions are not included [11]. $F(s)$ represents the transfer function of the loop filter. K_d is the combined gain of PFD and CP, and K_v is the sensitivity of the VCO. N is the division ratio of the MMD. The noise from the VCO, reference signal and CP is denoted $\phi_{n,VCO}(s)$, $\phi_{n,ref}(s)$ and $I_{n,CP}(s)$, respectively. The term $\phi_{n,DSM}(s)$, which is the DSM quantization noise in the phase domain, can be derived from (1) as

$$\phi_{n,DSM}(s) = \frac{j\pi f_{ref}}{\sqrt{3}Ns}\left(2\sin\frac{s}{j2f_{ref}}\right)^2 \tag{4}$$

where f_{ref} is the reference frequency [4]. The output phase noise of the fractional-N frequency synthesizer can be derived as

$$\begin{aligned}\phi_{n,RF}(s) &= \left[\phi_{n,ref}(s) + I_{n,CP}(s) - \phi_{n,DSM}(s)\right]H(s)\\ &\quad + \phi_{n,vco}(s)H_e(s)\\ &= \phi_{n,PLL}(s) - \phi'_{n,DSM}(s)\end{aligned} \tag{5}$$

where

$$\phi_{n,PLL}(s) = \left(\phi_{n,ref} + I_{n,CP}(s)\right)H(s) + \phi_{n,vco}H_e(s), \tag{6}$$

$$\phi'_{n,DSM}(s) = \phi_{n,DSM}(s)H(s), \tag{7}$$

$$H(s) = \frac{NK_vK_dF(s)}{Ns + K_vK_dF(s)}, \tag{8}$$

$$H_e(s) = \frac{Ns}{Ns + K_vK_dF(s)}. \tag{9}$$

The transfer functions $H(s)$ and $H_e(s)$ have a low-pass and a high-pass frequency response, respectively. According to (5), the noise $\phi_{n,ref}$, $I_{n,CP}$ and $\phi_{n,DSM}$ can be suppressed by the system outside the loop-bandwidth. The phase noise $\phi_{n,VCO}$ can be suppressed within the loop-bandwidth by the system.

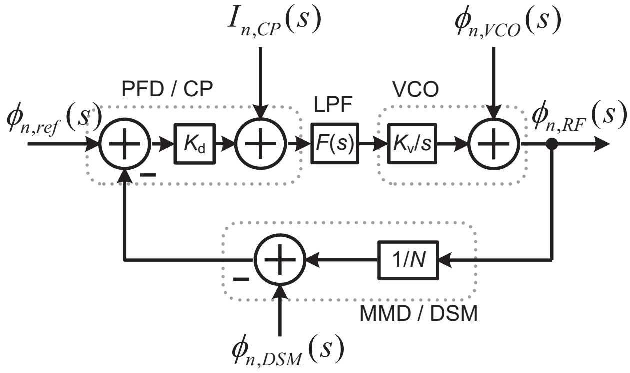

Fig. 3. Phase noise model of fractional-N frequency synthesizer.

Fig. 4 displays the noise cancellation model of the proposed pre-distortion technique in the time domain. Based on (5), the quadrature output signals in the time domain of the fractional-N frequency synthesizer are represented as

$$\begin{aligned}RF_I(t) &= \cos\left(2\pi f_c t + \phi_{n,RF}(t)\right)\\ &= \cos\left(2\pi f_c t + \phi_{n,PLL}(t)\right)\cos\left(\phi'_{n,DSM}(t)\right)\\ &\quad - \sin\left(2\pi f_c t + \phi_{n,PLL}(t)\right)\sin\left(\phi'_{n,DSM}(t)\right),\end{aligned} \tag{10}$$

$$\begin{aligned}RF_Q(t) &= \sin\left(2\pi f_c t + \phi_{n,RF}(t)\right)\\ &= \sin\left(2\pi f_c t + \phi_{n,PLL}(t)\right)\cos\left(\phi'_{n,DSM}(t)\right)\\ &\quad + \cos\left(2\pi f_c t + \phi_{n,PLL}(t)\right)\sin\left(\phi'_{n,DSM}(t)\right)\end{aligned} \tag{11}$$

where f_c is the central frequency of the RF signal, and

$$\phi_{n,RF}(t) = \mathrm{L}^{-1}\left\{\phi_{n,RF}(s)\right\}, \tag{12}$$

$$\phi_{n,PLL}(t) = \mathrm{L}^{-1}\left\{\phi_{n,PLL}(s)\right\}, \tag{13}$$

$$\phi'_{n,DSM}(t) = \mathrm{L}^{-1}\left\{\phi'_{n,DSM}(s)\right\}, \tag{14}$$

L^{-1} is the inverse Laplace transform. The output of the quadrature modulator can be then derived as

$$\begin{aligned}V_{out}(t) &= I_{pd}(t)RF_I(t) + Q_{pd}(t)RF_Q(t)\\ &= I_{pd}(t)\cos\left(2\pi f_c t + \phi_{n,PLL}(t)\right)\cos\left(\phi'_{n,DSM}(t)\right)\end{aligned}$$

$$- I_{pd}(t)\sin\left(2\pi f_c t + \phi_{n,PLL}(t)\right)\sin\left(\phi'_{n,DSM}(t)\right)$$
$$+ Q_{pd}(t)\sin\left(2\pi f_c t + \phi_{n,PLL}(t)\right)\cos\left(\phi'_{n,DSM}(t)\right)$$
$$+ Q_{pd}(t)\cos\left(2\pi f_c t + \phi_{n,PLL}(t)\right)\sin\left(\phi'_{n,DSM}(t)\right) \quad (15)$$

where $I_{pd}(t)$ and $Q_{pd}(t)$ are the pre-distorted $I(t)$ and $Q(t)$, respectively. To cancel out the quantization noise $\phi'_{n,DSM}(t)$ shown in (15), $I_{pd}(t)$ and $Q_{pd}(t)$ are designed as

$$I_{pd}(t) = I(t)\cos\left(\phi'_{n,DSM}(t)\right) - Q(t)\sin\left(\phi'_{n,DSM}(t)\right)$$
$$= \frac{1}{\sqrt{1+\tan^2\left(\phi'_{n,DSM}(t)\right)}}\left\{I(t) - Q(t)\tan\left(\phi'_{n,DSM}(t)\right)\right\}, \quad (16)$$

$$Q_{pd}(t) = Q(t)\cos\left(\phi'_{n,DSM}(t)\right) + I(t)\sin\left(\phi'_{n,DSM}(t)\right)$$
$$= \frac{1}{\sqrt{1+\tan^2\left(\phi'_{n,DSM}(t)\right)}}\left\{Q(t) + I(t)\tan\left(\phi'_{n,DSM}(t)\right)\right\}. \quad (17)$$

Applying (16) and (17) to (15) yields the output of the quadrature modulator as (18), which is shown at the bottom of the page. Equation (18) demonstrates that the quantization noise $\phi'_{n,DSM}(t)$ can be theoretically cancelled by the proposed architecture.

Based on (5) and (18), Fig. 5 presents quantization noise cancellation of a fractional-N frequency synthesizer using pre-distortion technique. The quantization noise pre-distorts the baseband signal. When this pre-distorted signal is used to modulate the RF carrier signal, the quantization noise in the carrier signal is cancelled out. Consequently, the signal-to-noise ratio (SNR) of the output modulation signal is greatly improved and the modulation quality exceeds that obtained without quantization noise cancellation.

2.4 Pre-distortion Filter

To achieve perfect cancellation of quantization noise, a well-designed digital pre-distortion filter is required. Based on (16) and (17), Fig. 6 presents the vectors of the original and pre-distorted signals. Pre-distorted signals are phase-rotated from the original signals by a phase of $\phi'_{n,DSM}(t)$. Therefore, the coordinate rotation digital computer (CORDIC) algorithm can be used to simplify the implementation of the digital pre-distortion filter [12]. Based on the CORDIC algorithm, the pre-distortion shown in (16) and (17) can be realized by iterating the following in the digital domain:

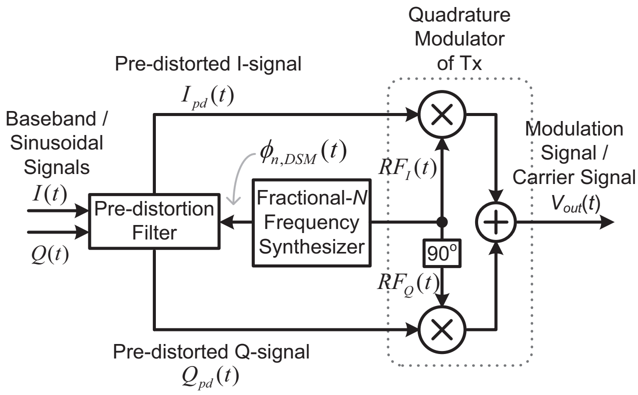

Fig. 4. Noise cancellation model of proposed pre-distortion technique.

$$I_{pd}[i+1] = I[i+1] = \frac{1}{\sqrt{1+2^{-2i}}}\left\{I[i] - Q[i]\sigma_i 2^{-i}\right\}, \quad (19)$$

$$Q_{pd}[i+1] = Q[i+1] = \frac{1}{\sqrt{1+2^{-2i}}}\left\{Q[i] + I[i]\sigma_i 2^{-i}\right\} \quad (20)$$

where $I[i]$, $I_{pd}[i]$, $Q[i]$, $Q_{pd}[i]$ are the sampled $I(t)$, $I_{pd}(t)$, $Q(t)$, $Q_{pd}(t)$ at the i^{th} step, respectively; and $\sigma_i = \pm 1$ is the direction of the phase rotation at the i^{th} step. Each iteration of (19) and (20) rotates the phase of the vector by $\tan^{-1}(2^{-i})$. Following a sufficient number of iterations, the accumulated phase rotation approaches the desired quantization noise

$$\phi'_{n,DSM} = \sum_{i=0}^{n} \sigma_i \tan^{-1}\left(2^{-i}\right). \quad (21)$$

$$V_{out}(t) = \cos\left(2\pi f_c t + \phi_{n,PLL}(t)\right)\Big\{ I(t)\cos^2\left(\phi'_{n,DSM}(t)\right) - Q(t)\sin\left(\phi'_{n,DSM}(t)\right)\cos\left(\phi'_{n,DSM}(t)\right)$$
$$+ Q(t)\cos\left(\phi'_{n,DSM}(t)\right)\sin\left(\phi'_{n,DSM}(t)\right) + I(t)\sin^2\left(\phi'_{n,DSM}(t)\right) \Big\}$$
$$+ \sin\left(2\pi f_c t + \phi_{n,PLL}(t)\right)\Big\{ Q(t)\sin^2\left(\phi'_{n,DSM}(t)\right) - I(t)\sin\left(\phi'_{n,DSM}(t)\right)\cos\left(\phi'_{n,DSM}(t)\right)$$
$$+ I(t)\sin\left(\phi'_{n,DSM}(t)\right)\cos\left(\phi'_{n,DSM}(t)\right) + Q(t)\cos^2\left(\phi'_{n,DSM}(t)\right) \Big\}$$
$$= I(t)\cos\left(2\pi f_c t + \phi_{n,PLL}(t)\right) + Q(t)\sin\left(2\pi f_c t + \phi_{n,PLL}(t)\right). \quad (18)$$

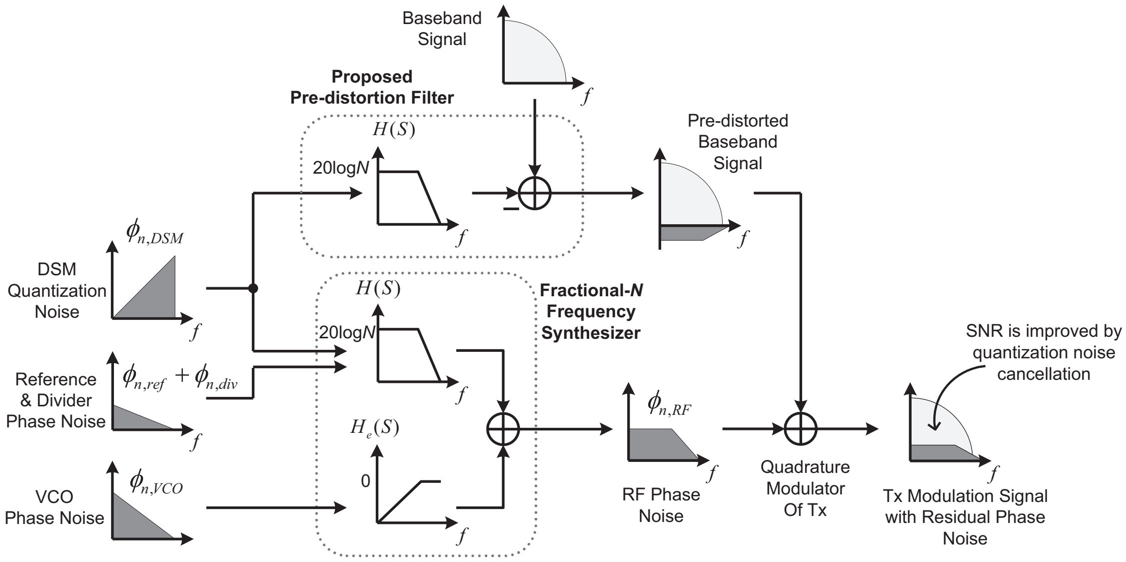

Fig. 5. Quantization noise cancellation of a fractional-*N* frequency synthesizer using pre-distortion technique.

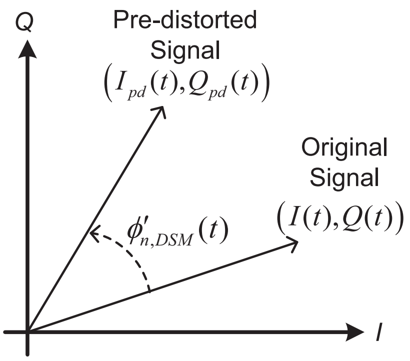

Fig. 6. Vectors of original and pre-distorted quadrature signals.

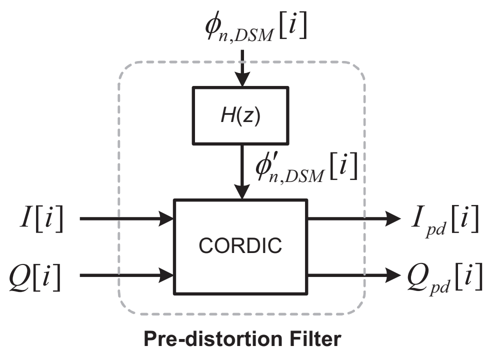

Fig. 7. Block diagram of proposed pre-distortion filter.

Since

$$\prod_{i=0}^{\infty} \frac{1}{\sqrt{1+2^{-2i}}} \approx 0.6073 \approx \frac{1}{2}+\frac{1}{2^4}+\frac{1}{2^5}+\frac{1}{2^6}, \quad (22)$$

(19) and (20) can be simplified as

$$I_{pd}[i+1] = \left(\frac{1}{2}+\frac{1}{2^4}+\frac{1}{2^5}+\frac{1}{2^6}\right) I[i+1], \quad (23)$$

$$Q_{pd}[i+1] = \left(\frac{1}{2}+\frac{1}{2^4}+\frac{1}{2^5}+\frac{1}{2^6}\right) Q[i+1] \quad (24)$$

where

$$I[i+1] = I[i] - Q[i]\,\sigma_i\,2^{-i}, \quad (25)$$

$$Q[i+1] = Q[i] + I[i]\,\sigma_i\,2^{-i}. \quad (26)$$

Equations (23) – (26) indicate that the CORDIC-based pre-distortion can be simply implemented using bit-shifters, adders and subtracters. Fig.7 displays the block diagram of the proposed pre-distortion filter, where two root-raised-cosine (RRC) filters are used for the pulse shaping of the baseband signal, and

$$H(z) = Z\{H(s)\} \quad (27)$$

is the digitized system-transfer function of the synthesizer. To simplify the implementation of $H(z)$, the proposed frequency synthesizer utilizes a first-order *R-C* loop filter, which makes the system transfer function $H(s)$ as a second-order transfer function. (8) can then be re-derived as

$$H(s) = \frac{2s\xi\omega_n}{s^2 + 2s\xi\omega_n + \omega_n^2} \quad (28)$$

where

$$\omega_n = \sqrt{\frac{K_V K_d}{NRC}}, \quad (29)$$

$$\xi = \frac{\omega_n}{2} RC. \quad (30)$$

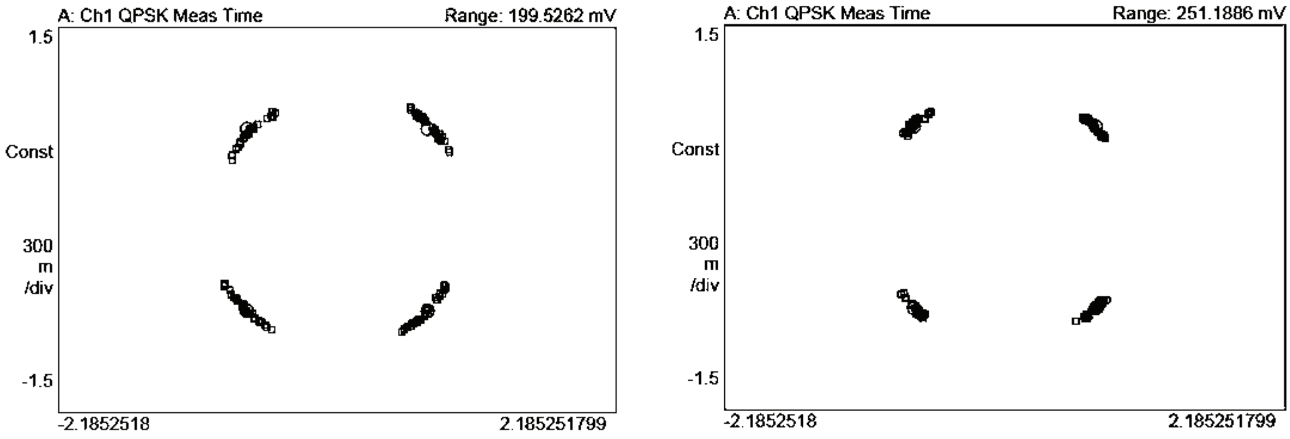

(a) (b)

Fig. 9. Measured constellation points of a 13 Mbps QPSK modulation signal (a) without and (b) with pre-distortion technique.

The digitized system-transfer function shown in (27) can then be derived as

$$H(z)=\frac{Az^2+Bz}{Cz^2+Dz+E} \tag{31}$$

where

$$A=2\xi\omega_n\sqrt{1-\xi^2}\,, \tag{32}$$

$$B=\omega_n e^{-\frac{\xi\omega_n}{f_{ref}}}\sin\left(\frac{\omega_n\sqrt{1-\xi^2}}{f_{ref}}\right)$$
$$-2\xi\omega_n e^{-\frac{\xi\omega_n}{f_{ref}}}\sin\left(\frac{\omega_n\sqrt{1-\xi^2}}{f_{ref}}+\cos^{-1}\xi\right), \tag{33}$$

$$C=\sqrt{1-\xi^2}\,, \tag{34}$$

$$D=-2\sqrt{1-\xi^2}\,e^{-\frac{\xi\omega_n}{f_{ref}}}\cos\left(\frac{\omega_n\sqrt{1-\xi^2}}{f_{ref}}\right), \tag{35}$$

$$E=\sqrt{1-\xi^2}\,e^{-\frac{2\xi\omega_n}{f_{ref}}}\,. \tag{36}$$

3. Experimental Results

Fig. 8 shows the implementation of fractional-N frequency synthesizer using pre-distortion technique. The frequency synthesizer of this work is a Peregrine product with a model number of PE335. The TRF3703-15 quadrature modulator and ROS-3050-819+ VCO are products of Texas Instruments (TI) and Mini-Circuits, respectively. The reference frequency and the operating frequency of the fractional-N frequency synthesizer is set as 20 MHz and 2 – 3 GHz, respectively. The fractional-N frequency synthesizer is designed with a 50 kHz loop bandwidth. The second-order DSM, channel selector, pre-distortion filter, and baseband signal generator are implemented using Xilinx Virtex-5 field-programmable gate arrays (FPGA).

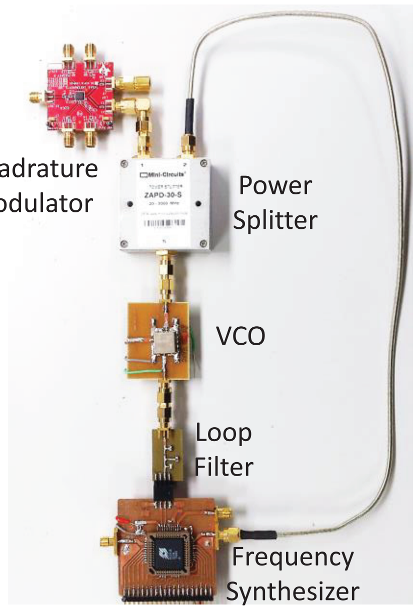

Fig. 8. Implementation of fractional-N frequency synthesizer using pre-distortion technique.

In the Tx mode, a 13 Mbps baseband signal is used to perform a QPSK modulation. Fig. 9 (a) and (b) presents the measured constellation points of the 13 Mbps QPSK modulation signal without and with pre-distortion technique, respectively. Without pre-distortion technique, the constellation points of the modulation signal are rotationally spreading out due to the considerable quantization noise. As the pre-distortion function is turned on to cancel the DSM quantization noise, the spreading of the 13 Mbps QPSK constellation points are improved and concentrated. These results indicate that the proposed pre-distortion technique improves the peak error vector magnitude (EVM) by more than 10 %.

In the Rx mode, 2 MHz sinusoidal signals replace the baseband signals to generate a CW as a carrier signal. Fig. 10(a) and (b) shows the measured output spectra and phase noise, respectively. The phase noise at an offset frequency of 1 kHz and 1 MHz is lower than -74 dBc/Hz and -101 dBc/Hz, respectively. The measurements indicate that the proposed pre-distortion technique works very well and improves the in-band and out-band phase noise of the carrier signal by approximately 6 dB and 10 dB, respectively. It can be found that there is almost no improvement at the moderate frequency offset. The main reason is that the frequency response of the digital pre-distortion filter is not completely identical to the one of the analog frequency synthesizer in both magnitude and phase. This non-ideal characteristic makes the improvement of the phase noise non-uniform over all the frequencies.

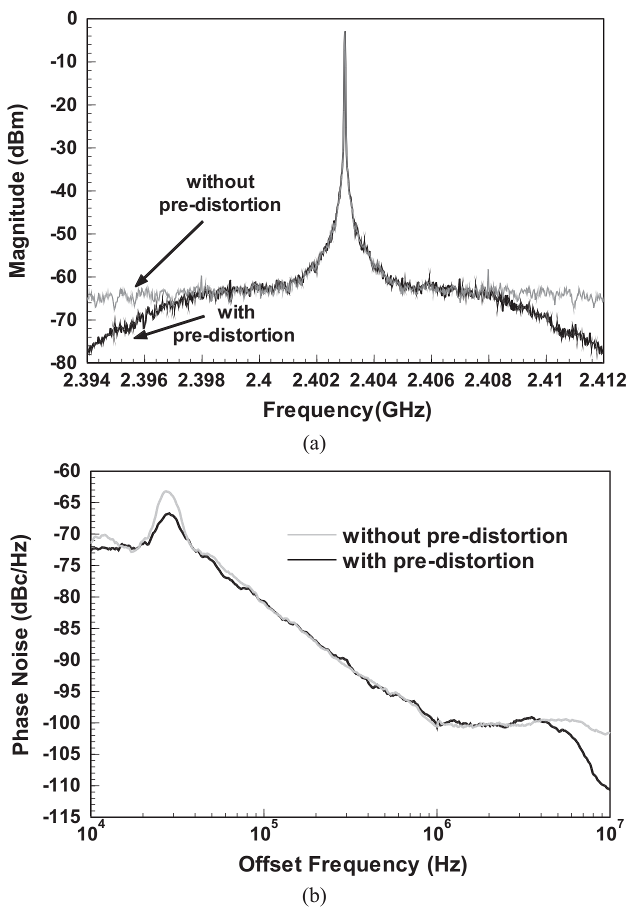

Fig. 10. Measured (a) spectra and (b) phase noise with and without pre-distortion technique.

Tab. 1 summarizes the performance of the fractional-*N* frequency synthesizer using the proposed pre-distortion technique. All of the measurements demonstrate that the proposed pre-distortion technique works perfectly with fractional-*N* frequency synthesizers. Tab. 2 presents the comparison of quantization noise cancellation techniques. The proposed pre-distortion technique achieves the higher out-band phase noise improvement. The remarkable phase noise improvement results in a 10 % EVM improvement when the carrier signal is modulated with a 13 Mbps QPSK signal. Comparing with the prior arts [6],[9], the proposed pre-distortion technique cancels out the DSM quantization noise with a much simpler circuitry and a lower operating frequency of the DSM.

Operating frequency	2 – 3 GHz
Reference frequency	20 MHz
Frequency resolution	305 Hz
Locking time	< 20 μs
Loop bandwidth	50 kHz
Phase noise	-74 dBc/Hz @ 1 kHz -101 dBc/Hz @ 1 MHz
EVM	5% (13 Mbps QPSK)

Tab. 1. Performance summary of the fractional-*N* frequency synthesizer using pre-distortion technique.

Reference	This work	[9]	[6]
Cancellation technique	Pre-distortion	Pre-distortion	Phase-interpolation
Number of DACs	0	0	1
High-capacity ROM	0	1	0
Operating frequency of DSM	20 MHz	105 MHz	20 MHz
Phase noise improvement	10 dB @10MHz	-	6 dB @10MHz
Modulation quality improvement	10 % (13 Mbps QPSK)	-	13 % (2.5 Mbps GFSK)

Tab. 2. Comparison of quantization noise cancellation techniques.

4. Conclusion

This work develops a novel pre-distortion technique for quantization noise cancellation of fractional-*N* frequency synthesizers. The proposed technique simply uses the inherent baseband-processing and modulation of a wireless system to cancel out the DSM quantization noise. It therefore reduces hardware complexity. In the Tx mode, the pre-distortion technique improves the EVM of a 13 Mbps QPSK signal by more than 10 %. In the Rx mode, the pre-distortion technique improves the phase noise of the carrier signal by 6 dB and 10 dB at 30 kHz and 10 MHz offset frequency, respectively. The locking time of the fractional-*N* frequency synthesizer is shorter than 20 μs. These remarkable measurements reveal that the proposed synthesizer architecture using pre-distortion technique is very suitable for advanced wireless systems.

Acknowledgements

The authors would like to thank the National Science Council (102-2221-E-327-006) for providing research funding.

References

[1] MUSCHALLIK, C. Influence of RF oscillators on an OFDM signal. *IEEE Transactions on Consumer Electronics*, 1995, vol. 41, no. 3, p. 592 - 603.

[2] CHRISTOFFERS, N., KOKOZINSKI, R., KOLNSBERG, S., HOSTICKA, B. J. High loop-filter-order sigma-delta fractional-*N* frequency synthesizers for use in frequency-hopping-spread-spectrum communication-systems. In *Proceeding of the 2003 IEEE International Symposium on Circuits and Systems*. 2003, p. 216 - 219.

[3] SHU, K., SANCHEZ-SINENCIO, E., MALOBERTI, F., EDURI, U. A comparative study of digital ΣΔ modulators for fractional-*N* synthesis. In *Digest of the 8th IEEE International Conference on Electronics, Circuits and Systems*. 2001, p. 1391 - 1394.

[4] PENG, K. C., HUANG, C. H., Li, C. J., HORNG, T. S. High performance frequency hopping transmitters using two-point delta-sigma modulation. *IEEE Transactions on Microwave Theory and Techniques*, 2004, vol. 52, no. 11, p. 2529 - 2535.

[5] PENG, K. C., WU, P. S. High Performance fractional–*N* frequency synthesizer using a two-point channel selection technique. In *Digest of the 2009 IEEE Asia-Pacific Microwave Conference*. 2009, p. 1275 - 1278.

[6] PENG, K. C., LIN C. C., CHAO C. H. A novel three-point modulation technique for fractional-*N* frequency synthesizer applications. *Radioengineering*, 2013, vol. 22, no. 1, p. 269 – 275.

[7] ZHANG, L., YU, X., SUN, Y., PHEE,W., WANF, D., WANG, Z., CHEN, H. A hybrid spur compensation technique for finite-modulo fractional-*N* phase-locked loops. *IEEE Journal of Solid-State Circuit*, 2009, vol. 44, no. 11, p. 2922 - 2934.

[8] SHEKHAR, S., GANGOPADHYAY, D., WOO, E. C., ALLSTOT, D. A 2.4-GHz extended-range type-I ΣΔ fractional-*N* synthesizer with 1.8-MHz loop bandwidth and -110 dBc/Hz phase noise. *IEEE Transactions on Circuits and Systems II, Express Briefs*, 2011, vol. 58, no. 8, p. 472 - 476.

[9] WANG, H. *New Strategies for Low Noise, Agile PLL Frequency Synthesis*. Ph.D. dissertation. London (UK): Dept. Electronic & Electrical Eng. Univ. College London, 2009.

[10] HAYKIN, S. *Communication Systems*, 5th ed. John Wiley & Sons, 2009.

[11] ZHAO, B., LIAN, Y., YANG H. A low-power fast-settling bond-wire frequency synthesizer with a dynamic-bandwidth scheme. *IEEE Transactions on Circuits and Systems I, Regular Papers*, 2013, vol. 60, no. 5, p. 1188 - 1199.

[12] AGGARWAL, S., MEHER, P. K., KHARE, K. Scale-free hyperbolic CORDIC processor and its application to waveform generation. *IEEE Transactions on Circuits and Systems I, Regular Papers*, 2013, vol. 60, no. 2, p. 314 - 326.

About Authors ...

Kang-Chun PENG was born on February 18, 1976, in Taipei, Taiwan. He received the B.S.E.E., M.S.E.E. and Ph.D. degrees from the National Sun Yat-Sen University, Kaohsiung, Taiwan, in 1998, 2000 and 2005, respectively. He is currently an Assistant Professor with the Department of Computer and Communication Engineering, National Kaohsiung First University of Science and Technology, Kaohsiung, Taiwan. He is also the treasurer of the IEEE Microwave Theory and Techniques Society (IEEE MTT-S) Tainan Chapter. His current research interests are in the area of delta-sigma modulation techniques, injection-locking techniques, wideband frequency synthesizers and coherent demodulators.

Yan-Ru LU was born on August 18, 1986, in Kaohsiung, Taiwan. He received the B.S.E.E. degree from the National Kaohsiung University, Kaohsiung, Taiwan, in 2010. He received the M.S.E.E. degrees from the National Kaohsiung First University of Science and Technology, Kaohsiung, Taiwan, in 2012. He is currently with the Chung Shan Institute of Science and Technology, Taoyuan County, Taiwan, R.O.C.

Zhi-Hong HUANG was born on September 1, 1987, in Yunlin, Taiwan. He received the B.S.E.E. degree from the National Kaohsiung Marine University, Kaohsiung, Taiwan, in 2009. He received the M.S.E.E. degrees from the National Kaohsiung First University of Science and Technology, Kaohsiung, Taiwan, in 2011. He is currently with the Syncomm Technology Corp., Hsinchu City, Taiwan, R.O.C.